

Positron-annihilation study of silver irradiated by energetic protons or neutrons

R. H. Howell

Lawrence Livermore Laboratory, Livermore, California 94550

(Received 22 July 1980; revised manuscript received 16 March 1981)

To study the relationship of recoil energy to damage production we have irradiated well-annealed samples of silver at room temperature with energetic protons from 4.5 to 22.5 MeV or D-T fusion neutrons up to maximum fluences of $6 \times 10^{17} p \text{ cm}^{-2}$ and $\times 10^{17} n \text{ cm}^{-2}$. Positron-annihilation analysis including both lifetime and Doppler-broadening profile data was used to determine the characteristics of the surviving defects. The trapping-rate data exhibit a strong nonlinear fluence dependence, which may be due to radiation annealing of the damage. There is also clear evidence of a threshold recoil energy below which the defect survival efficiency is very low. This threshold is determined to be between 50- and 100-keV recoil energy.

I. INTRODUCTION

Defect production and survival depend on the energy of the primary recoil atom. The detailed dependence can give information on the type of defects produced in the cascade region. The survival probability is also temperature dependent. At temperatures above stage three, there are defects which are both the result of migration of point defects and residual structure produced directly from the irradiation, while at lower temperatures point-defect migration is inhibited. Low-energy recoils are seen to produce defects at nearly 100% of the rate predicted by a modified Kinchin-Pease model¹; however, this efficiency drops to between 20 and 30 % when the recoil energy is greater than a few keV.^{2,3}

In irradiations performed above the activation temperatures for migration of point defects, the relationship between recoil energy and defect survival is changed. The active, mobile defects produced by low-energy recoils tend to migrate either to sinks and disappear or to traps where they grow into larger, more stable defects. These effects can lead to a higher efficiency for the survival of defects produced in the initial cascade region and a lower survival efficiency for point defects if the concentration of sinks is sufficiently high. The effects of defect survival at room temperature have been studied in copper.^{4,5} It was found that defect survival was low for defects produced by recoils below 55 keV and that those surviving tended to be related to sample impurities which served as nucleation centers.⁶

In silver the survival efficiency for defects as a function of recoil energy has been studied in low-temperature proton irradiations.¹ Silver irradiated at

room temperature by self-ions or by D-T neutrons has been studied in transmission-electron microscopy (TEM) and the threshold for cascade production⁷ and the defect survival probability⁸ have been determined. Since the parameters for the interaction of the silver recoil have been observed over a wide range of conditions, we undertook this study of the irradiation characteristics of silver at room temperature to further illustrate the issue of defect survival dependence on recoil energy.

II. EXPERIMENTAL METHOD

Detailed descriptions of the apparatus and analysis technique used to obtain the lifetime and Doppler-broadening data have been provided in Refs. 4 and 5. The lifetime data were obtained in a conventional fast coincidence system with instrumental resolution of 160 psec full width at half maximum (FWHM). The source was 15- μCi ^{22}Na deposited on a 1-mg/cm² nickel foil. Source annihilations contributed about 5% of the total counts with a 400-psec lifetime component. Doppler-broadening data were obtained with a lithium-drifted germanium detector with 1.23-keV resolution at 511 keV. The data were reduced to the generally used parameters S and W which are defined in Ref. 9. The parameters S and W correspond to the peak (I_p) and wing (I_c) parameters of that work.

The result of a positron measurement is an average of the sample characteristics weighted by the positron distribution in the sample. For positrons from a ^{22}Na source this distribution falls exponentially from the source location to the end of the positron range with an attenuation length in silver of

19.57 μm .¹⁰ Consequently the positron measurements which are reported here are heavily weighted to the conditions near the surface and each sample surface will give distinct data. In some samples the experimental parameters change rapidly as a function of depth (for example, proton energy in the proton irradiations). Consequently the positron distribution must be weighted by the changing values of the experimental quantity. This weighting has been approximated by choosing to specify the sample condition at the depth to which one-half of the positrons penetrate. The effect of averaging over the range of the positron is small in the neutron-irradiated samples where the variation of the damage with depth is slight. The pronounced variation of proton energy with depth in the sample results in a stronger effect for proton-irradiated samples.

Samples were prepared from disks 12.7 mm in diameter and 0.37 mm thick of MRC Marz grade polycrystalline silver which were annealed at 600 °C for 6 h in an atmosphere of argon and 1% hydrogen. The samples when removed from the furnace were bright and showed no visible signs of oxidation. Those samples which were reserved for proton irradiation were then electropolished to a final thickness of 0.305 ± 0.003 mm. Both polished and unpolished samples were positron analyzed and only a single lifetime value was observed. Similarly no differences in Doppler-broadening characteristics were evident in the polished and unpolished samples. The values found in these analyses were taken as the bulk annihilation values in subsequent models.

The samples were irradiated by protons at the Lawrence Livermore Cyclograaff facility. For each irradiation the protons passed through a stack of three samples so that each sample was irradiated by the same number of protons of different energy. For each fluence two sets of samples were separately irradiated so that two samples with identical proton-energy profiles were available. The positron source was then sandwiched between matching samples in a symmetric manner. The proton energy incident on the front face of the first sample was 22.5 ± 0.01 MeV with a FWHM of 0.015 MeV. After passing through all of the samples the proton beam had an energy of 4.5 MeV and a Gaussian energy distribution with 1.2-MeV FWHM.¹¹ In Fig. 1, the proton energy and damage energy cross section are graphed as a function of depth of penetration into the sample stack. The proton energy is the average proton energy. The values of the proton energy at the sample surfaces are 22.5, 18.0, 12.5, and

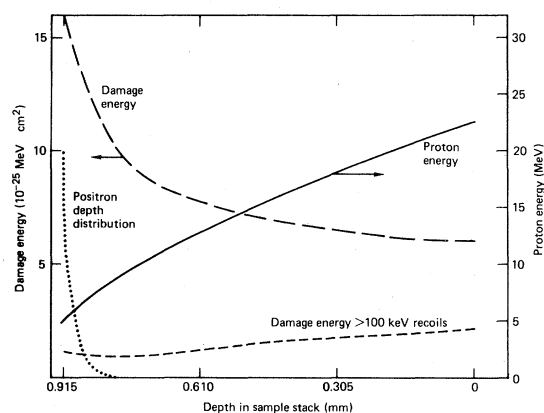


FIG 1. Proton energy and damage energy as a function of the depth of penetration into the silver samples. In the experiment protons entered from the right with an initial energy of 22.5 MeV. As the protons penetrated the samples the proton energy was degraded to a final value of 4.5 MeV for the exiting beam. The variation in the damage energy cross section results from the variation in the proton energy. The arbitrarily normalized positron depth distribution of a ^{22}Na source placed at the rear surface of the sample stack is also shown.

4.5 MeV calculated using the methods of Ref. 12.

The proton beam was rastered over a 0.317-cm^2 circular collimator directly in front of the samples so that a spatially uniform dose was delivered to the irradiated area. The average current density was $3 \mu\text{A cm}^{-2}$ during most of the runs. Heat deposited in the samples from energy lost from the proton beam was removed through an alcohol-cooled brass heat sink in which the samples were spring loaded. The outer diameter of the samples were in good contact with the heat sink and the face of the last sample was in full contact with the surface of the sink. The maximum temperature difference between the irradiated part of the sample and the heat sink is calculated to be about 2 °C for the geometry and beam current used in this experiment. The heat sink temperature was held at -5 °C during the runs. After irradiation the samples were allowed to warm to ambient temperature at which they were stored until the time of measurement.

Sample dosimetry was done by measuring the integrated charge deposited in the heat sink behind the last sample. A low bias (100 V) was held between the collimator and the heat sink so that secondary electron emission was suppressed.

Neutron irradiations were done with D-T fusion neutrons from the rotating target neutron source at Lawrence Livermore Laboratory (RTNS-I). This

accelerator provides an intense, spatially small source of fusion neutrons which are emitted isotropically. All samples were irradiated simultaneously with samples close to the source receiving higher doses than those farther away. Samples were kept in pairs with set distances between each pair to obtain the desired dose distribution. In the irradiation geometry the dose rate varied from 3×10^{11} to $6 \times 10^8 \text{ n cm}^{-2} \text{ sec}^{-1}$. The samples were kept at 15°C during the irradiation and then stored at ambient temperature until measurement. The neutron dose was measured for each sample by measuring the activation in niobium foils placed at each sample position. For those samples near the source, foils were placed before and after the sample so that any spatial variation in the neutron fluence was measured. In the closest samples the fore-aft fluence variation was less than 15% of the average dose of nearly $10^{17} \text{ n cm}^{-2}$. During positron analysis the positron source was sandwiched between the inner surfaces of the pairs of samples.

In both irradiations high levels of radioactive ^{106m}Ag , half-life 8.4 days, were produced. This isotope decays producing multiple cascade gamma rays all highly correlated in time. Consequently, the samples were stored after irradiation for a several month period before the first measurements were made. During this time the ^{106m}Ag activity decayed to a low level. The samples remained radioactive with low levels of ^{108}Ag and ^{110}Ag both of which are long lived. The final levels of residual radiation were minor when compared to the intensity of the positron source used so that no correction to the positron analysis was necessary for this effect.

III. RESULTS

A. Positron measurements

Doppler-broadening and lifetime measurements were made for the complete set of neutron-irradiated samples. For proton-irradiated samples the same types of data were obtained with pairs of samples irradiated to equal fluence. For the high proton energy the positron source was at the front surface of the first sample in the stack and for the low proton energy the positron source was at the back surface of the last sample in the stack. The regions sampled therefore were those irradiated by protons of average energies of 22 and 5.7 MeV. Lifetime measurements were made at one fluence with the positron source at each face of each sample providing data for all the energies between the ex-

tremes. The Doppler-broadening data were reduced to the commonly used peak and wing parameters $S = I_v$, $W = I_c$ defined in Ref. 9. The lifetime spectra were analyzed in terms of three models: the single-lifetime model, the independent two-lifetime model, and the single-trap model.

The results of the single-lifetime analysis of the lifetime data and the S and W parameters of the Doppler-broadening data for the neutron and proton sample sets are shown in Fig. 2. The lifetime obtained for well-annealed silver is $140 \pm 3 \text{ psec}$. This is in excellent agreement with the results ($138 \pm 3 \text{ psec}$) of Ref. 13. The single-lifetime values increase with fluence to saturation for the proton-irradiated sample sets. The saturation value depends on the energy and type of radiation used to damage the sample. The lowest saturated lifetime was obtained from the low-energy-proton sample set. The highest lifetime was obtained from the un-

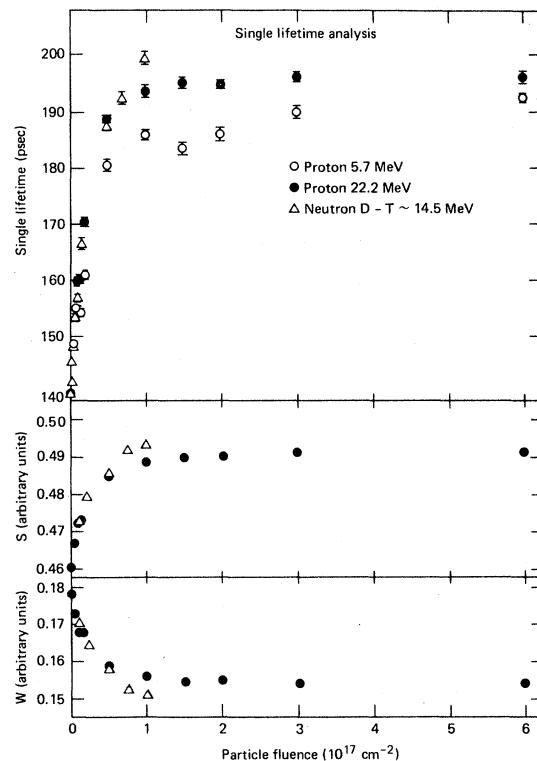


FIG 2. Values of the broadening parameters S and W , and the values for a single-lifetime-model fit to the positron data for silver irradiated by protons at 5.7 or 22 MeV or D-T fusion neutrons. The lifetime values are the result of a single-lifetime fit to the lifetime spectrum. The definitions of the S and W parameters are given in the text. The data at the highest fluences appear to have reached saturation; however, the saturation values are different for each of the sources.

saturated neutron sample set. In the S and W parameter data the increase to saturation for proton-irradiated samples and the greater increase for the neutron-irradiated samples are similar to the lifetime data.

The same lifetime spectra were also analyzed with a model which included two independent, freely varying lifetimes. It was found that the lifetime of the long-lived component was longer than the lifetime obtained from a single-lifetime analysis and that the intensity of the long-lived component was never greater than 85% in the saturation regions. The value of the short-lived component was near the single-lifetime value for low-fluence values and was as low as 60 psec in the saturation region. These are the classic characteristics of the trapping model and the trapping rate can be extracted from these analyses. The results of the two-lifetime analysis suggest that the saturation which is observed in the single-lifetime analysis is a saturation of the trapping rate. If the saturation were due to all the positrons annihilating at trapping sites then the analysis would produce 100% intensity of the long-lived component and a long-lifetime value consistent with the results of a single lifetime analysis. This is just the behavior which was observed in samples of deformed silver to be discussed later.

Since the trapping model as used with the results of an independent two-lifetime model applies to

these spectra, the trap lifetime and trapping rates can be determined by fitting the trapping model to the spectra directly. The advantage in doing so is that the value of the free lifetime can be fixed to the value determined by measurement of well-annealed material while the trapping rate and trap lifetime vary freely. This constraint is physically reasonable and is also needed to get trapping rates from the two-lifetime model. This analysis results in less scatter in the values of the trap parameters, especially in those spectra where the contribution of the trap-related components is small. Trapping model and independent two-lifetime analysis of the same spectra as analyzed by a single lifetime were done. In general the quality of the fit obtained with either of the multiple lifetime models was identical for each spectrum with the chi-squared per degree of freedom always near 1. However, for spectra in the region intermediate to annealing and saturation, the quality of the fit improved using either the trapping model or the two-lifetime model as compared to the single-lifetime model. The value of the chi-squared per degree of freedom was reduced by as much as 40% and there was a noticeable improvement in the residual spectrum.

The trapping rate results of a single-trap analysis are shown in Fig. 3. The average proton energies are 22.2 and 5.7 MeV, respectively. The analysis of the samples was done with the bulk lifetime fixed at

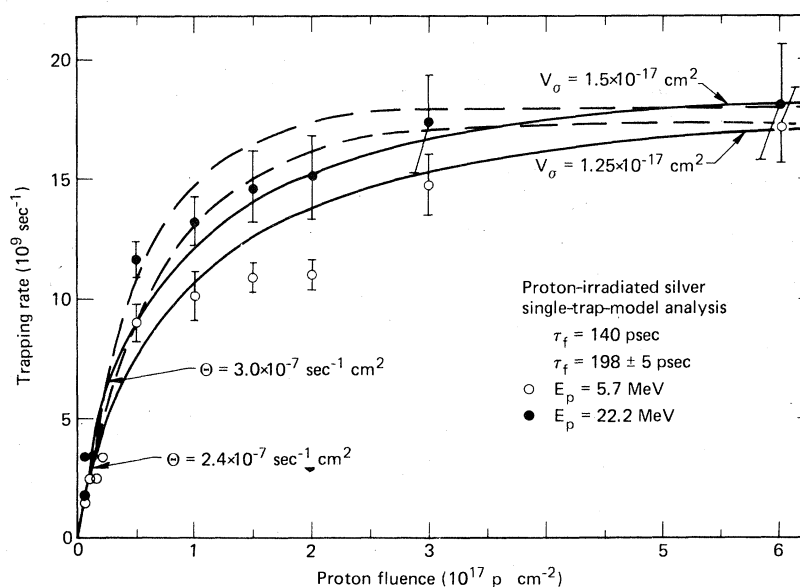


FIG 3. Trapping-rate values derived from a single-trap model of the lifetime data from silver irradiated by protons with 5.7 or 22-MeV energy. The nonlinear fluence dependence of the trapping rate, seen at both proton energies, has been modeled by two radiation annealing models: one including annealing-volume changes (solid lines) and one without volume changes (dashed lines).

140 psec and the trapping rate and trap lifetime varying freely. The contribution from annihilations in the source was fixed at 0.048% and 405 psec as determined in analysis of spectra taken with well-annealed silver. Both the trap lifetime and the trapping rate for the high-proton-energy irradiation and the low-proton-energy irradiation are shown. The data for the two proton energies are similar. The trap lifetime was found to be the same regardless of the irradiation energy or fluence. The average and standard deviation about the mean of all of the lifetime values is 198 ± 5 psec.

In the simplest model the fluence dependence of the trapping rate would be expected to be a linear function of fluence. It is evident that the fluence dependence of the trapping rate for both energy irradiations is distinctly nonlinear and in fact seems to be tending to a saturation value at the highest fluences. This is the same result as obtained from the two-lifetime model.

The results of a single-trap model analysis of the lifetime data from the neutron-irradiated samples are shown in Fig. 4 with an expanded fluence scale. The trapping-rate analysis was done with the bulk lifetime fixed at 140 psec and the trapping rate and trap lifetime varying freely. The source contribution was fixed to the same values as in the proton analysis. The fluence dependences of the trap lifetime and the trapping rate are qualitatively the same as that observed in the proton-irradiated samples, in-

cluding the tendency for the trapping rate to be nonlinear. The average and deviation about the mean of the trap lifetimes is 200 ± 2 psec. Neutron irradiations were not obtained at a high enough fluence to see full saturation in the trapping rate as was observed in the proton-irradiated samples.

In the data at the higher fluences for both the neutron and the proton irradiations the deduced trap lifetime is significantly longer than the lifetime value obtained from a single-lifetime fit. This is especially true for the low-energy-proton-irradiated samples. A comparison of the residual spectra showed pronounced structure when the data were analyzed with a single lifetime and no observable structure when the data are analyzed with the trapping model or two-lifetime model. This is additional evidence that the observed saturation is the result of a saturation in the density of traps and not in the rate of positron trapping. If the rate of positron trapping were saturated, then every positron would be trapped and only one lifetime, that of the positron in the trap, would have been observed in the saturated spectrum.

Studies which are analyzed in terms of average parameters, such as the Doppler-broadening peak parameter S , or the average lifetime, depend on the saturated value of the measurement to define the value of the totally trapped state. We attempted to obtain trapping rates from the lifetime data in this study by forcing a fit to the spectra with the trap-

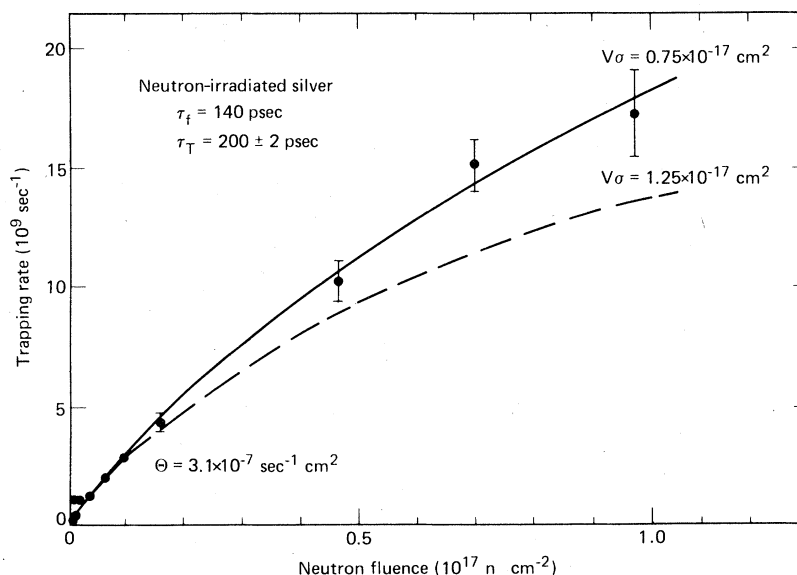


FIG 4. Trap lifetime and trapping-rate values derived from a single-trap model of the lifetime data from silver irradiated by D-T fusion neutrons. The nonlinear trapping-rate dependence is modeled by radiation annealing as was done in Fig. 3. Only fits of the variable-volume model are shown. Note that the fluence scale is changed from that in Fig. 3.

ping model fixing both the bulk lifetime and the trap lifetime to the values found in the single-lifetime analysis. This procedure resulted in significantly increased values of chi-squared in the fit and a degraded residual spectrum. The nonlinear behavior of the trapping rate persists in this analysis, displaying a qualitatively similar dose dependence to the best-fit values obtained with a freely determined trap lifetime. Thus it is with some confidence that the trapping-rate values are presented as distinctly nonlinear with respect to the sample dose and that the trap lifetime is longer than the values found in a single-lifetime analysis of the highest dose samples for both irradiation sources.

The trapping rate as a function of proton energy at constant fluence was obtained with the positron source placed at each surface in the sample stack. Samples from two irradiations at equal fluence ($2 \times 10^{16} p \text{ cm}^{-2}$) were measured in a symmetric source sample geometry. The results are presented in Fig. 5 as a function of depth in the stack of silver samples. The trapping rate varies only slightly over the range of proton energies. This result is similar to that found for copper irradiated under similar conditions. The detailed investigation of the energy dependence of the trapping rate was carried out at one proton fluence. However, since the fluence dependence of the trapping-rate data shown in Fig.

3 is identical we expect that a similar proton-energy dependence would be obtained at any fluence.

Defects produced in deformation have similar positron annihilation responses to those produced by irradiation. To compare these processes we introduced defects into well-annealed silver stock by cold rolling to thickness reductions of up to 50%. The Doppler-broadening profiles and lifetime spectra obtained for these samples are shown in Fig. 6. The Doppler-broadening and the single-lifetime analysis show signs of saturation for deformations of greater than 10%. The trap lifetime determined in a single-trap-model analysis of the lifetime spectra was found to be constant varying about the average value 199 ± 3 psec which is consistent with the single-lifetime values at large deformation. This trap lifetime is very close to that found in the irradiated samples. In the analysis of highly deformed samples the two-lifetime model resulted in 100% intensity of the long-lifetime component and the single-trap model resulted in trapping rates which increased without convergence. Thus the same analysis technique which results in trapping-rate saturation in irradiated samples results in positron saturation by 100% trapping in the deformed samples. The trapping rates obtained from a single-trap-model analysis of the lifetime spectra and analysis of the Doppler-broadening data using the values at the

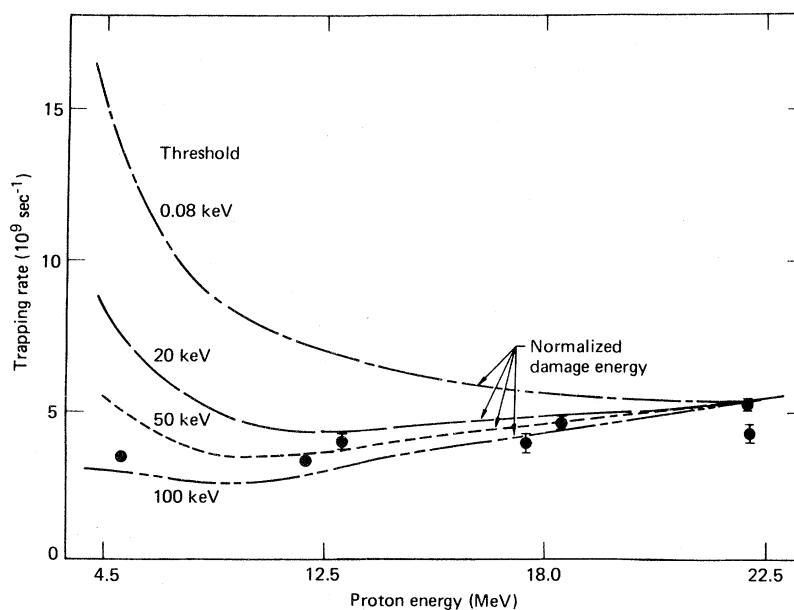


FIG 5. Trapping-rate values for samples irradiated by protons of different energies to the same dose ($2 \times 10^{16} p \text{ cm}^{-2}$). The curves are damage-energy calculations with various thresholds set in the recoil distribution, normalized to the trapping rate at high proton energy. The trapping-rate values are quantitative and can be used to select one of the threshold values from the damage-energy calculation.

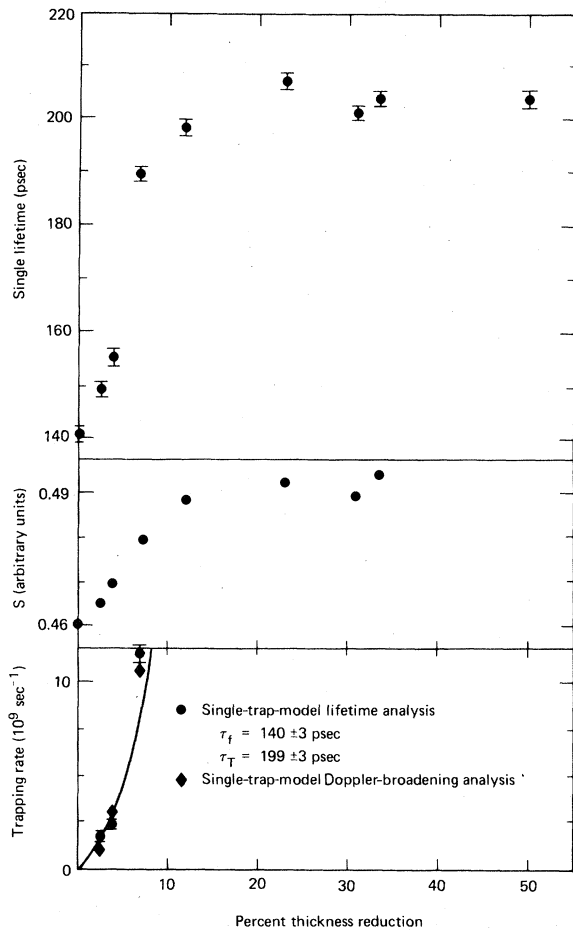


FIG 6. Single-lifetime Doppler-broadening parameters and deduced trapping-rate results for deformed silver. The saturation values for both the Doppler-broadening parameter and the single lifetime are higher than those for the irradiated samples. Analysis of these data with a single-trap model yields a constant trap lifetime of 199 ± 3 psec. The line through the trapping-rate data is calculated from values for the trapping-rate cross section from Ref. 9.

highest deformation values as trap values are both shown. The curve is calculated using values from Ref. 14 in which the trapping rate per unit defect was obtained. The normalization has been adjusted to account for the present value of the free lifetime τ_f .

B. Damage calculations

Calculations of the defect production rate in silver irradiated by protons or neutrons were based on calculated energy distributions of the silver recoils.

The recoil spectra were calculated from a combination of experimental data and nuclear models. Neutron-produced recoils were calculated from the tabulated experimental data for neutron scattering and reactions. The proton recoil spectra were derived from proton elastic scattering calculated with the nuclear optical model, and proton inelastic reactions parametrized by data of equilibrium and pre-equilibrium neutron emission. Other less important parts of the proton reaction cross section were ignored. A detailed description of these calculations may be found in Refs. 15–17.

Not all of the recoil energy is lost in damage-producing interactions. The damage energy, which is the portion of the recoil energy available for defect production, is calculated from the recoil energy using a parametrization of the theory of Lindhard.⁸ The total damage-energy cross section is obtained by integrating the damage energy for all recoil energies. The displacement rate ν at some recoil energy T is obtained from the distribution of damage energy, E_{dam} , using a modified version of the Kinchin-Pease model given by

$$\nu(T) = \begin{cases} 0, & T < E_d \\ 1, & E_d \leq T \leq 2.5E_d \\ 0.8E_{\text{dam}}(T)/2E_d, & 2.5E_d \leq T \end{cases}$$

where E_d is the average displacement threshold which is 39 eV for silver.

In the production of defects from high-energy recoils there are transitions corresponding to the onset to cascade production (1–3 keV)¹ and multiple cascade production (30–100 keV).^{7,8} A model which only included damage energy from recoils above a threshold set in this energy region was used to describe the relationship between positron trap rate and neutron and proton damage in copper. In experiments on silver irradiated at low temperature the efficiency of the defect survival was observed to drop for recoil energies above the cascade production threshold. The efficiency at high-recoil energy was found to be 30% of the low-energy value with the transition region occurring at 1–3 keV in the recoil spectrum.¹

The results of calculations of the damage-energy cross section integrated from a low-recoil-energy threshold and from thresholds set in the keV region of the recoil spectrum are presented in Table I. The rate of displacements per atom (dpa) is related to the damage-energy cross section by a constant factor also given in Table I.

TABLE I. Calculated damage energy for protons and neutrons on silver. The damage-energy values are calculated for several thresholds in the recoil-energy distribution. Contributions from recoils below the threshold energy are not included in the damage energy. Also given is the trapping-rate-production cross section determined for protons and neutrons in the present experiment. The values of the trapping-rate-production cross sections are expected to be proportional to the damage energy. For this to be so, a threshold between 50 and 100 keV must be chosen in the damage-energy calculation. The normalization of the damage energy to displacement rate was calculated using an average displacement threshold energy of 39 eV. To convert damage energy to dpa/(p cm⁻²), multiply by 1.025 × 10⁴.

Threshold (kev) E_n (MeV)	100	75	50	20	0.08	
	Damage energy (10 ⁻²⁵ cm ² MeV)				Trapping-rate cross section (10 ⁻⁷ sec ⁻¹ cm ²)	
14.5 E_p (MeV)	2.0	2.1	2.1	2.2	2.3	3.1
25	2.5	2.6	2.7	2.9	5.6	
20	2.0	2.1	2.2	2.5	6.1	3.0
15	1.4	1.6	1.8	2.2	7.4	
10	1.0	1.3	1.6	2.5	8.9	
5	1.0	1.6	2.3	4.1	17.6	2.4

IV. DISCUSSION

A. Defect trapping

Defects in many metals and alloys have been analyzed by positron annihilation. Several defects have been specifically identified as traps including vacancies, dislocations, and voids. The vacancy formation energy in silver has been measured by observing the Doppler-broadened annihilation spectra as a function of sample temperature¹⁹ The annealing behavior and absolute trapping rate of irradiation produced vacancies have been measured.¹³ Also, the trapping cross section for silver has been measured for dislocations produced in deformation.¹⁴ Thus, silver has been demonstrated to trap positrons at two recognized defects and, while trapping at voids has not been observed in silver, there is no reason to doubt that it would occur in void-containing samples.

The behavior of all of the positron-annihilation results for the proton- and neutron-irradiated silver clearly shows the effects of positron trapping. Only one trap lifetime was observed in any of the damaged samples in the present experiment. The lifetime values, 198 ± 5 and 200 ± 2 psec are in reasonably good agreement with the monovacancy lifetime, 208 ± 5 psec determined in Ref. 13; however, it is below the value 230 ± 15 psec for the ex-

tended defect observed in that work.

The short value of the trap lifetime is a puzzling aspect of both the present data and also data obtained on copper under similar conditions. These experiments were performed at temperatures above the stage-three transition and point defects are all highly mobile. In addition high-energy irradiations and deformations produce complex systems of defects. It has been suggested that complex defects, such as dislocations produced by deformation, may be decorated by single vacancies at jogs which serve as the final trap site.²⁰ This interpretation would explain the features of the present data and offers the possibility of a correlation of the positron results obtained from radiation- and deformation-induced defects.

B. Recoil threshold

The survival of defects produced at the time of irradiation and the resulting traps can be different for low-energy-recoil events and those with higher energy. Both the proton-energy dependence and the comparison of the proton- and neutron-trapping cross sections suggest that recoils below some high-energy threshold do not result in defects which trap positrons.

Evidence for a high-threshold value is found in the proton-energy dependence of the trapping rate

seen in Fig. 5. The calculated damage energies are normalized to the data at the highest proton energy. The low-threshold damage-energy calculation is clearly much too large in the low-proton-energy region. This might be expected as the low threshold includes low-energy recoils which produce individual point defects and the irradiation occurred at a temperature at which these defects are highly mobile and would quickly migrate to defect traps or sinks. The best threshold appears to be in the recoil energy region between 50 and 100 keV.

Other evidence of a high-energy threshold in the recoil spectrum is found by comparing the trapping-rate cross sections and damage-energy calculations for protons and neutrons found in Table I. The damage-energy cross-section values are proportional to the trapping-rate cross-section values only when the damage energy is calculated with a threshold of 50 to 100 keV. Consequently, the proton-energy dependence and proton-neutron comparisons give the same threshold values. The threshold value is similar to that found for copper in a similar experiment, and is higher than the recoil energy 1 keV, at which the efficiency of damage survival in the cascade drops.

C. Trapping-rate properties

In the proton-irradiated samples there is a saturation level in the trapping rate. The positron-annihilation data presented here are consistent in determining that the trapping rate has an upper limit. The evidence for this includes: The damage dependence of the average values determined by single-lifetime analyses and Doppler-broadening analysis is consistent in all cases. The saturation result was consistently seen in lifetime analysis with either an independent two-lifetime model or a single-trap model fit to the data. The trap lifetimes determined in those analysis are greater than the single lifetime determined for the same data. The trap lifetimes are remarkably consistent. And lastly, 100% positron trapping was seen in measurements on highly deformed samples, strongly suggesting that the trapping-rate saturation is not an artifact of the analysis technique.

A saturation value of the trapping rate must be related to a saturation limit in the concentration of the traps. An alternate explanation, that the saturation of the trapping rate is the result of the dynamics of the positron migration to the trap, can be rejected. The diffusion model predicts an increase in trapping rate at high defect concentrations.²¹

If the saturation and nonlinearity in the trapping

rate is due to the defect concentration, then there must be some mechanism which is limiting the concentration of surviving defects. Radiation annealing of individual point defects has been observed²² in silver irradiated at low temperature by 500-keV self-ions where the self-ion annealing volume was found to be $6 \times 10^{-16} \text{ cm}^3$.

Since the irradiations and analysis of the silver samples in this experiment were done at room temperature, the individual Frenkel pairs will have all annealed in less time than that compared with the irradiation time. Thus the effect which is observed here must be due to the overlapping of the volumes of the multiple cascade regions distributed along the path of the recoil.

The survival of defects in overlapping annealing volumes can be modeled on the basis of a constant volume for the annealing process or with an annealing volume which depends on the previous history of the sample.²³ In a model with changing volume the effective volume would shrink as the dose increased. The functional form of the positron trapping rate K for each of these models is

$$K = \frac{\alpha}{2V} [1 - \exp(-2V\sigma\phi)]$$

for a constant annealing volume, and

$$K = \theta\phi / (1 + V\sigma\phi)$$

for a dose-dependent annealing volume, where V is the annealing volume, σ is the recoil cross section, ϕ is the particle fluence of the primary radiation, and $\theta = \alpha\sigma$ is damage-production cross section normalized to the positron measurement, i.e., the trapping-rate cross section. The predictions of these models are shown in Fig. 3 for the proton-irradiation data.

The choice of either of the radiation-annealing models does not affect the size of the trapping-rate cross section; however, the size of the volume is model dependent. The variable-volume model produces a volume twice as large as the constant-volume model. Shape differences between the models are found at intermediate fluence levels while the values for the annealing volume and cross section are determined by the behavior at the fluence limits.

In Fig. 3 the constant volume model does not describe the overall dose dependence of the trapping rate as well as the changing-volume model. This is especially true for the low-energy-proton data. Consequently we will use the changing-volume model in the following discussion.

Fits of the changing-volume model have been made to the proton and neutron data, and the

TABLE II. Calculated average and maximum recoil energies E_R , the recoil cross section σ_R , and consequent radiation-annealing volume V for protons and neutrons. The recoil attenuation cross section is obtained by multiplying σ_R by $5.74 \times 10^{22} \text{ cm}^{-3}$. The product of the radiation volume- and recoil-production-attenuation cross section $V\sigma$ is fixed by the comparison of the radiation-annealing model to the trapping-rate data. The values of the average recoil energy and annealing volume depend on the lower threshold in the recoil spectrum and have been given for the same thresholds as in Table I.

Threshold (keV)		100			75		
E_p	E_R^{max}	σ_R (barns)	V^a (10^{-17} cm^3)	$E_{R\text{av}}$ (MeV)	σ_R (barns)	V^a (10^{-17} cm^3)	$E_{R\text{av}}$ (MeV)
Neutrons							
15	0.545	1.6	7.94	0.16	1.9	6.75	0.15
Protons							
5	0.182	1.16	18.3	0.13	2.05	10.0	0.1
10	0.364	0.94	25.0	0.14	1.43	17.0	0.12
15	0.545	1.27	18.0	0.15	1.51	15.0	0.15
20	0.730	1.5	16.0	0.2	1.60	15.0	0.19
25	0.900	1.61	16.0	0.23	1.70	14.0	0.23

^aVolumes deduced from empirical values of $V\sigma = 0.75^{-17} \text{ cm}^2$ for neutron-irradiated samples and $V\sigma = 1.25 \times 10^{17}$ and $1.5 \times 10^{-17} \text{ cm}^2$ for samples irradiated by 5.7- and 22-MEV protons, respectively. $V\sigma$ values at other proton energies were derived by linear extrapolation.

values for the initial volume and cross section for producing traps have been obtained in each case. The values of θ are found in Table I and $V\sigma$ in Table II. The values of the product $V\sigma$ and of θ can be determined unambiguously; however, the values of V depend on the value of the recoil cross section.

The recoil cross section depends on the lower limit set in the recoil energy just as in the damage-energy calculations. Consequently, it is necessary to calculate the volume for each of the thresholds which might be applicable, since the same threshold may not apply to defect annealing as to defect production. Table II contains values for the cross section, average recoil energy, and annealing volume for both irradiation sources and several recoil-energy thresholds. Since the product of $V\sigma$ was nearly the same for both high- and low-energy-proton irradiations it was assumed to vary linearly in the calculations for all proton energies in Table II.

Both proton and neutron irradiations at room temperature give volumes which are less than that ($6 \times 10^{-16} \text{ cm}^3$) determined for 500-keV self-ions at low temperature. The smaller volume determined in this experiment versus the self-ion irradiation is due to two effects: First, the average energy of the recoiling silver atoms in the present experiment is always much less than the 500 keV used in the

self-ion irradiation. Second, the higher temperature in the present experiment allows the point defects produced far from the cascade region to anneal thermally without assistance from radiation.

In self-ion irradiation the volume is roughly equal to the recoil range cubed. The volumes determined in this experiment, using a high-recoil-energy threshold, are several times larger than the average recoil range cubed but are generally less than the cubed range at the maximum recoil energy. Consequently, the volume is roughly the size of the multiple cascade region. This is not so for the smaller volumes calculated with low-recoil-energy thresholds. Also the calculated volumes for the lowest-energy thresholds for proton irradiations are much smaller than the corresponding volume obtained from the neutron irradiation. The comparison of the volumes determined in both irradiations may be taken as additional evidence of an effective threshold in the many-keV-energy region of the recoil-energy distribution.

The volumes, calculated with a high-recoil-energy threshold, for the proton irradiated samples are comparable, one to another, but they are consistently larger than the corresponding volumes determined for neutron-irradiated samples. This cannot be explained by the energy distribution of the high-energy portion of recoil spectrum as it is very similar for the energetic recoils for neutrons and pro-

TABLE II. (Continued).

σ_R (barns)	50 V^a (10^{-17} cm^3)	$E_{R^{av}}$ (MeV)	σ_R (barns)	20 V^a (10^{-17} cm^3)	$E_{R^{av}}$ (MeV)	σ_R (barns)	0.08 V^a (10^{-17} cm^3)	$E_{R^{av}}$ (MeV)
2.36	5.4	0.14	2.70	4.7	0.13	4.4	3.0	0.07
3.72	5.7	0.08	11.1	1.9	0.04	6×10^3	0.003	7×10^{-5}
2.15	11.0	0.09	6.17	3.8	0.04	1.5×10^3	0.015	3×10^{-4}
1.93	12.0	0.13	4.28	6.0	0.04	6×10^2	0.04	3×10^{-4}
1.90	13.0	0.17	3.46	7.0	0.07	4×10^2	0.061	4×10^{-4}
1.90	13.0	0.22	2.95	8.0	0.14	2×10^2	0.12	5×10^{-4}

tons. The difference may be due to the presence in the proton-irradiated samples of many low-energy recoils which produce point defects which participate in the annealing process. The difference could also be due to the difference in dose rates between the proton and neutron irradiations. A lower dose rate would allow a longer time for thermal annealing of partially bound damage associated with the cascade. The maximum neutron dose rate was less than that for the proton irradiations. There are no clear indications from the present data to choose which of these possibilities affect the annealing volume; however, they are the strongest differences between the two irradiations and either could have an effect on the volume.

Since the trap lifetime is nearly the same in the deformation studies and the irradiation studies, it is tempting to assign the same identification regions containing dislocations to the two traps, and to use the trapping-rate per defect determined from the deformation studies to calculate the defect concentration of the irradiation-produced traps. This approach would not be justified if the defects are significantly different. The deformed samples did not show any sign of defect density saturation in contrast to the irradiated samples. Even so, the correlation of irradiation trapping rate to dislocation density does have value as an indication of the overall consistency of the positron measurements, especially if the trapping rate is related to some common defect feature such as the strain field. The lifetime of

the defects would be determined by the vacancies bound to jogs.²⁰ The dislocation density per recoiling particle can be calculated using the trapping-rate cross section θ , and the trapping rate to dislocation density normalization determined in Ref. 14, corrected to correspond to bulk annihilation rates determined in this work. Choosing a threshold of 100 keV in the recoil energy the length of dislocation line per recoil can be calculated. The value is 1.1×10^{-6} cm per recoil for all cases: D-T fusion neutrons and high- and low-energy protons.

This length dislocation corresponds to loop sizes that are smaller than the radiation annealing volume but the same as the overall dimensions of the visible clusters in a cascade region⁷ determined in TEM. If the radiation-induced damage is assumed to be in a circular loop as in Ref. 7 then this calculation would predict only one loop of about 3.5×10^{-7} cm in diameter per recoil. This is roughly the defect size inferred in Ref. 13 from the temperature dependence of the positron trapping rate. For this to be the case there must be a low efficiency of conversion of displacements into dislocations, about 0.1 if the displacement rate is calculated with a 100-keV threshold and less for lower-recoil-energy-threshold values. This efficiency is lower than the 0.3 value determined in low-temperature experiments or 0.17 calculated from Ref. 8 for room-temperature irradiation. However, in self-ion irradiation of silver at room temperature⁸ the efficiency of defect survival observed by resistivity changes dropped to $\frac{1}{3}$ the

low-temperature value. Combining this loss with that measured at low temperature for defects in the cascade region results in a total efficiency of 0.1, in good agreement with the present experiment.

This lower efficiency may be due to annealing effects above the stage-three transition temperature or to some difference in the traps produced in deformation as compared to those from irradiation. In particular the use of the same unit trapping rate for both line dislocations and loops may be inappropriate. However, the overall consistency of the results obtained using positron analysis and those from TEM and resistivity studies may be taken as an indication of the strong similarity of the positron-annihilation mechanism in the deformation and radiation damage measurements.

V. SUMMARY

Well-annealed silver has been irradiated by energetic protons or by D-T fusion neutrons at room temperature up to a maximum fluence of $6 \times 10^{17} p \text{ cm}^{-2}$ or $1 \times 10^{17} n \text{ cm}^{-2}$. The characteristics of the damage introduced by irradiation have been determined by positron-annihilation analysis using both the lifetime and Doppler-broadening data. A threshold of 50–100 keV in the recoil-energy distribution is required if the surviving damage from all the irradiation data is to be described by damage-energy calculations. This threshold effect has been seen before in copper irradiated under similar conditions.

The positron trapping rate was determined and a strong nonlinear dependence on fluence, tending to saturation, was observed for all irradiation conditions. The fluence dependence was explained by an irradiation-annealing model in which the volume was a function of the fluence level, shrinking as the fluence was higher. An annealing model with a fixed volume did not describe the data as well. The size of the volume is consistent with the values of the range of the recoiling silver atoms and with data determined independently by low-temperature self-ion irradiation annealing. The size of the volume, which depends on the lower cutoff in the recoil spectrum used in determining the cross section for participating recoil events, also indicates that there is a damage survival threshold in the keV recoil-energy range. These data, together with studies of cold deformation of silver, yield similar values for the trap lifetime in all cases; however, the defect survival rate for the irradiation process is rather low when calculated by normalizing to the deformation data.

ACKNOWLEDGMENT

The author would like to acknowledge many useful conversations with M. Guinan and also R. Haight for his careful reading of this manuscript. This work was performed under the auspices of the U. S. Department of Energy by the Lawrence Livermore Laboratory under Contract No. W-7405-ENG-48.

¹K. L. Merkle, R. S. Averback, and R. Benedek, *Phys. Rev. Lett.* **38**, 424 (1977).

²J. B. Roberto, C. E. Klabunde, J. M. Williams, R. R. Coltman, M. J. Saltmarsh, and C. B. Fulmer, *Appl. Phys. Lett.* **30**, 509 (1977).

³M. W. Guinan and C. E. Violet, *Symposium on Neutrons 10–40 MeV* (National Technical Information Service, Springfield, Va., 1977), p. 361.

⁴R. H. Howell, *Phys. Rev. B* **18**, 3015 (1978).

⁵R. H. Howell, *Phys. Rev. B* **22**, 1722 (1980).

⁶R. H. Howell (unpublished).

⁷R. L. Lyles and K. L. Merkel, *Radiation Effects and Tritium Technology for Fusion Reactors* (National Technical Information Service, Springfield, Va., 1976), Vol. 1, p. 161.

⁸K. L. Merkle and R. S. Averback, *Fundamental Aspects of Radiation Damage in Metals* (National Technical Information Service, Springfield, Va., 1976), p. 127.

⁹S. Mantl and W. Triftshäuser, *Phys. Rev. B* **12**, 1645 (1978).

¹⁰Allen N. Goland, *Fundamentals Aspects of Radiation Damage in Metals* (National Technical Information Service, Springfield Va., 1975), p. 1107.

¹¹C. Tschälar, *Nucl. Instr. Methods* **61**, 141 (1968).

¹²M. W. McNaughton, United Kingdom Atomic Authority Report No. AERE-R7072, HMSO, London (unpublished).

¹³P. Hautjärvi, J. Johansson, A. Vehanen, J. Yli-Kaupila, P. Gerard, and C. Minier (unpublished).

¹⁴J. Baram and M. Rosen, *Phys. Status Solidi* **16**, 263 (1973).

¹⁵C. M. Logan, J. D. Anderson, and A. K. Mukherjee, *J. Nucl. Mater.* **48**, 223 (1973).

¹⁶A. M. Omar, J. E. Robinson, and D. A. Thompson, *J. Nucl. Mater.* **64**, 121 (1977).

¹⁷C. M. Logan and E. W. Russell, LLL Report No. UCRL-52093, National Technical Information Service, Springfield, Va. (unpublished).

¹⁸M. T. Robinson, *Nuclear Fusion Reactors* (British Nuclear Energy Society, London, 1970), p. 364.

- ¹⁹J. L. Campbell, C. W. Schulte, and J. A. Jackman, J. Phys. F 7, 1985 (1977).
- ²⁰L. Smedskjaer, M. Manninen, and M. Fluss, J. Phys. F 10, 2237 (1980).
- ²¹W. Brandt, R. Paulin, and C. Dauwe, Phys. Lett. 48A, 480 (1974).
- ²²R. S. Averback and K. L. Merkle, Phys. Rev. B 16, 3860 (1977).
- ²³A. Sosin and W. Bauer, *Studies in Radiation Effects in Solids*, edited by G. Dienes (Gordon and Breach, New York, 1969), Vol. 3, p. 153.